Journal of Engineering Science and Technology
Vol. 20, No. 3 (2025) 751 - 764


# TORSIONAL PERFORMANCE OF PERFORATED SQUARE HOLLOW STEEL BEAMS: NUMERICAL INVESTIGATION

RASHAD R. JAWAD[1], ALI A. KHAMEES[2], ALI A. AL-RAMMAHI[3,*]

[1]College of Engineering, University of Summer, Nasiriya, Iraq
[2]College of Engineering, Thi Qar University, Nasiriya, Iraq
[3]Al-Furat Al-Awsat Technical University, Najaf Technical Institute, Najaf, Iraq
*Corresponding Author: ali-alremahi@atu.edu.iq

## Abstract

The main purpose of steel beam holes is to decrease weight or to allow for the passage of electrical or sanitary conduits. Therefore, improving a steel beam's capacity without increasing its weight or cost is its biggest problem. The goal of the study was to create a 3D finite element model to describe and examine the torsional behavior of a SHS beam that has a side hole. The experimental findings of the earlier researchers confirmed and calibrated the finite element model. Regarding the final torsional capacity, failure mode, and torque-angle of twisting reaction, the model accurately agrees. A comparison with experimental data, which showed a maximum difference ratio based on the ultimate load of less than 18% for all models taken into consideration, validated the accuracy of the numerical analysis. The form, quantity, and kind of holes in the square hollow steel beam's sides were the subject of a parametric analysis. To lessen the weight of the model, the twisting behavior of models with rectangular, slanted, consecutive, and intersecting apertures was also shown and examined. The findings show that the final torque strength of the square hollow steel beam models is greatly impacted by the existence or absence of a hole. When the hole in the side of the beam emerged, the final capacity dropped from 18.3% to 31.9%. With the lateral buckling mode, every model failed.

Keywords: Beam, Numerical torsional investigation, Square beam, Steel beam, Perforated beam.

## 1. Introduction

Over the last few decades, Hollow Section has found extensive use in structural applications around the globe due to the many advantages it offers [1]. Engineers and architects have relied on steel hollow and tubular members throughout construction history due to their advantages over open sections. Some benefits include low drag coefficient, weight, useable interior space, economic terms, decreased protection needs, intrinsic attractiveness, and high torsional rigidity [2]. Metal hollow section members are perfect for practical torsional member applications due to their high torsional stiffness. One typical structural component is the thin-walled hollow section, which may be made using either the hot-rolling or cold-forming techniques. The cold-forming process is famous for improving mechanical qualities, including yield stress and tensile strength. It may be achieved by either cold-rolling or press-braking. However, it is also known to decrease ductility [3].

There are many different reasons why thin-walled steel hollow sections could have perforations, incisions, or holes incorporated into them [4]. These include mechanical maintenance, accessibility needs, electrical connections, plumbing services, and many more [3]. When such holes are present, the capacity of steel members may decrease. Several factors, such as the size, position, and quantity of holes, determine the magnitude of this decrease [5].

In the past few decades, researchers from many parts of the globe have examined the effects of cold forming on the behaviour of materials. While cold-formed steel hollow members have been the subject of numerous compression and bending investigations, their behaviour under torsion has received comparatively little attention. Perforations, also known as cuts or holes, can serve multiple purposes in structural applications, including girders, beyond improving the strength-to-weight ratio. These encompass a wide range of concerns, including aesthetics, the ease of maintenance of building utilities, and the connection of secondary components. However, the unforeseen effects of perforations might change the failure process and reduce structural capabilities [6]. Pham's studies explored the elastic buckling of perforated steel plates and members subjected to in-plane shear pressures at different angles [7].

The effects of eccentrically placed holes were further investigated, and approximation equations for the shear buckling coefficient were provided. Square and rectangular hot-rolled carbon steel plates were investigated for their plastic and elastic behaviours under shear stress by Pellegrino et al. [8]. Factors such as perforation size, location, and plate slenderness were considered. Wanniarachchi and colleagues [5] investigated the shear behaviour of lipped channel beams having non-circular web perforations, including square, rectangular, and elliptical shapes. The investigation created new shear design equations for perforated beams following a literature review of existing ones. According to Pham et al. [9], a collection of design equations for shear-perforated channel sections was produced. The Direct Strength Method (DSM), a more contemporary technique, was the foundation for these channel section formulas. It is worth mentioning that the majority of the study discussed before focused on plates and open section members. One torsional experiment with perforated hollow parts and one with closed sections were published in the literature by Ridley-Ellis et al. [6]. Considering the centre circular hole situated mid-length of the member, the findings from torsion testing on perforated hot-rolled and cold-formed steel were published. Also, the supplied

design suggestions for round hollow section members with hot-finished holes punched into them.

Devi et al. [10] attempted to examine the torsional behaviour of square hollow sections (SHS) with circular holes. Moreover, the corresponding minimum yield and tensile stresses for the YSt-310 cold-formed steel tube members used in this investigation are 310 MPa and 450 MPa, respectively. They looked at how different hole characteristics affected the torsional strength of SHS components. The holes' quantity, dimensions, and positioning are all relevant considerations. Unperforated and perforated cold-formed YSt-310 components were first tested in an experimental program to determine their material properties and torsional performance. Afterward, tested finite element (FE) models were used for parametric analysis in the Abaqus commercial program [11]. In their computational investigation, Devi and Singh [4] used a finite element model to check how stiffened perforation affected the torsional capacity of members with perforations in thin, lean duplex, metallic semi-elliptical hollow sections. Four stiffener configurations—horizontal, vertical, rectangular frame, and ring alignment—were investigated to fit a single circular hole onto the member's flat component. The researchers set out to determine how several geometric parameters, such as the circumference, thickness, and anchoring length, affected the torsional strength of a single perforated circular element.

This research aimed to evaluate the torsional performance of steel SHS members with different hole shapes. The effect of perforation characteristics on the torsional strength of square hollow section members made of steel was examined in this study. Perforation features include the quantity, kind, and form of holes. Another method to investigate how weight loss affected torsional behaviour was to rearrange the structural components and remove part of the material. A three-dimensional model was built using ABAQUS software. The correctness of the model was calibrated and verified by comparing the results to the author's earlier work [12, 13]. The findings from the finite element analysis provided several suggestions for predicting the torsional capacity of square hollow section members made of perforated steel.

## 2. Specimens' Clarification

The ten full-scale square hollow steel (SHS) models utilized in this study each have a clear span of 3000 mm, as seen in Fig. 1. Measurements of the models' cross-section are 200 × 200 mm in width and 10 mm in thickness. Models are designated by a symbol that indicates the number, kind, or form of the holes. For example, the R label designates the reference SHS beam model, denoted by the symbol (R). TH also stands for the triangular aperture. Details about the specimen and the meanings of the model name symbols are compiled in Table 1.

The reference model had no holes, while the rest only had holes. Holes with an area of 40,000 mm2 were taken, as this is the measurement used in most real steel beams, representing approximately 3.5% of the beam lateral area. Also, the proposed opening shapes are the most commonly used shapes. The hole's area was fixed for all models. Also, the total area remained the same when the number of circles increased. The successive vertical and inclined holes were placed to reduce the model's weight, as they represent 26% of the lateral area of the model, while the intersecting holes represented approximately 35% of the lateral area.

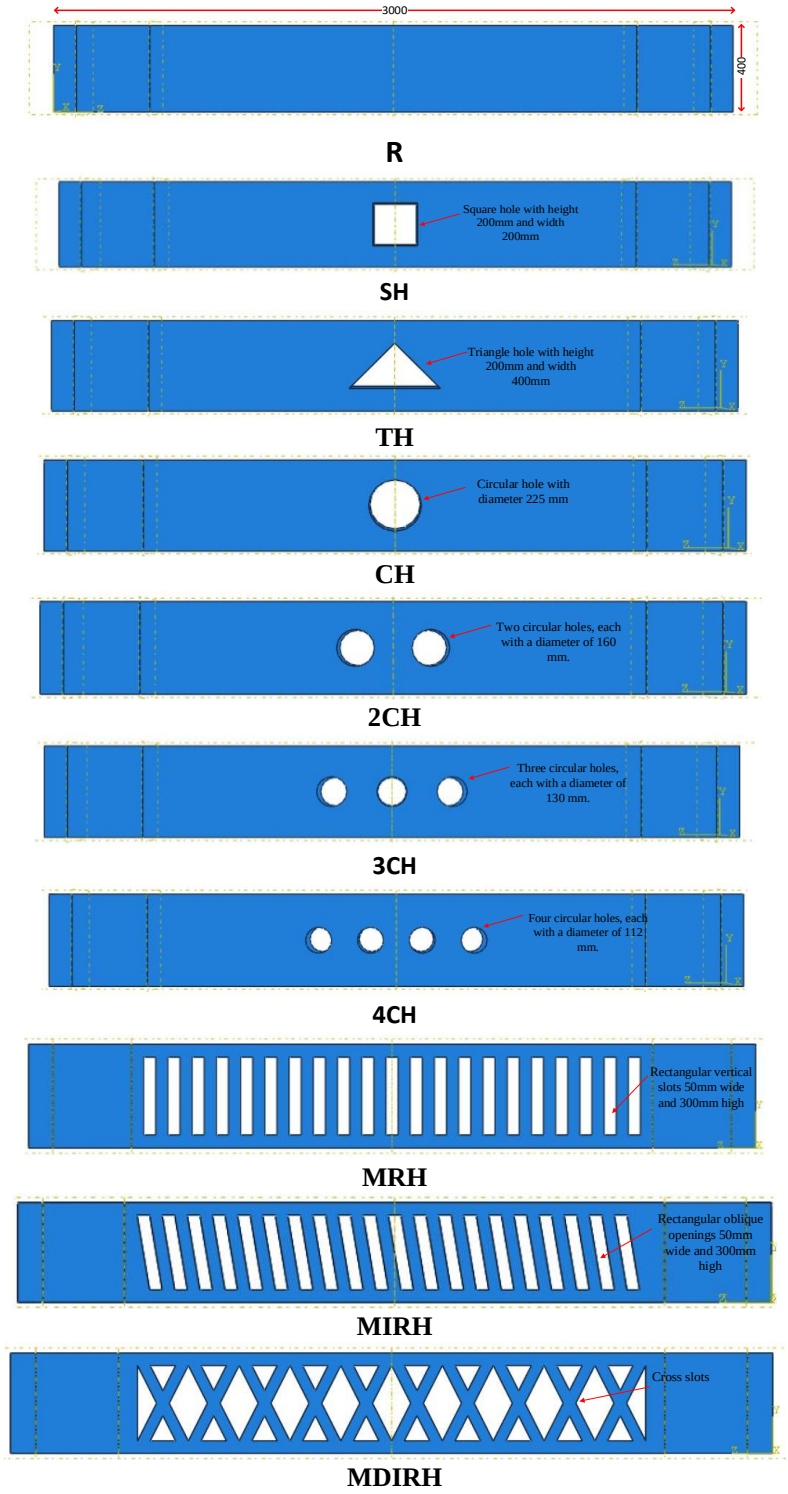


**Fig. 1. Models' dimensions and details.**

**Table 1. Models' dimensions.**

| Specimen Designations | Hole shape | Holes' dimension, mm | Notes |
|---|---|---|---|
| R | Non | Non | Reference model without hole |
| SH | Square | 200 (width) ×200 (length) | Square hole with a total area of 40,000 $mm^2$ |
| CH | Circle | 225 (diameter) | Circular hole with a total area of 40,000 $mm^2$ |
| TH | Triangle | 200 (height) × 400 (width) | A triangular hole with a total area of 40,000 $mm^2$ |
| 2CH | Circle | 160 (diameter) | Two circular holes with a total area of 40,000 $mm^2$ |
| 3CH | Circle | 130 (diameter) | Three circular holes with a total area of 40,000 $mm^2$ |
| 4CH | Circle | 112 (diameter) | Four circular holes with a total area of 40,000 $mm^2$ |
| MRH | Rectangle | 50 (width) ×300 (height) | Multi–rectangular holes |
| MIRH | Inclined rectangle | 50 (width) ×300 (height) | Multi-incline rectangular holes |
| MDIRH | Cross | --- | Multi-double incline rectangular hole |

## 3. Square Hollow Steel Beam FE Model

As a result of using ABAQUS / CAE version 6.12-3 technology, a 3D finite element model was developed. The model comprised three different sections, as seen in Fig. 2. These included a square steel hollow section beam and two stiff parts responsible for the twisting load. The steel hollow section beam and stiff twisting parts were modeled using a ten-node quadratic tetrahedron, allowing enhanced surface stress visualization. After trying several types, it was noted that this type of element represents the model perfectly. It was using the connection limitations that the two stiff twisting parts held on to the square hollow steel section beam. The simulation modeled the beam made of a square hollow steel section as pin-to-pin support. Both stiff twisting parts were subjected to the load in a manner that was consistent throughout. General Static is the kind of analysis that considers all essential irregularities throughout the simulation.

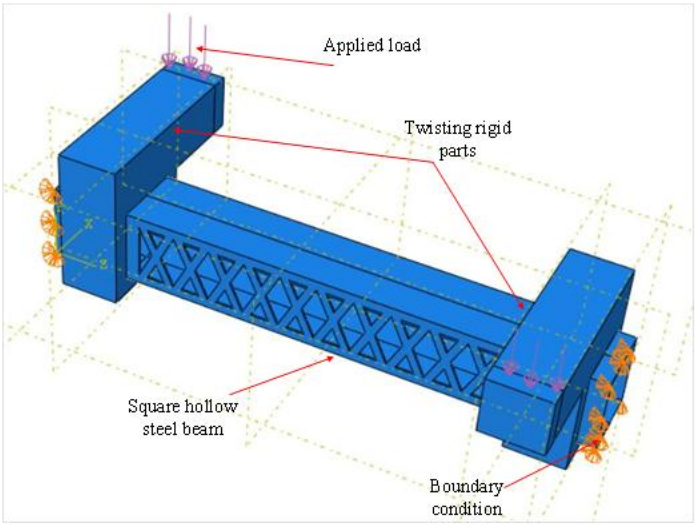


**Fig. 1. Square hollow steel section beam FE model.**

### 3.1. Materials characteristics and mesh

To get comparable results, the attributes of the defined models must be in complete agreement with the test specimens. As shown in Fig. 3, the stress-strain curve of the materials' properties has been established. A square hollow section steel beam and the two twisting parts have both been measured to have a steel modulus of 205 gigapascals per square inch. On the other hand, the Poisson Ratio has been determined to be 0.3 for all steel variations. It is indispensable to choose the sizes of the elements to achieve convergence of the findings. In this study, the number of components was altered to get the same behavior for both the models and the specimens that were evaluated regarding the failure mechanism and the failure angle of twisting. A convergence analysis was conducted on the steel beam model with a square hollow section to determine a suitable mesh density. A reduction in the mesh size, which has a significant impact on the outcomes, is the practical means by which this may be accomplished. This effect is due to the accuracy of the numerical analysis results when the mesh elements' sizes are reasonably small. As shown in Fig. 4, the optimal dimension for the square hollow section steel beam was 25 millimeters. This was accomplished by decreasing the mesh size from 100 to 10 millimeters by modeling the beam with the same material attributes. When the same amount of stress was applied to all the square hollow section steel beams, the mid-span twisting angle was measured.

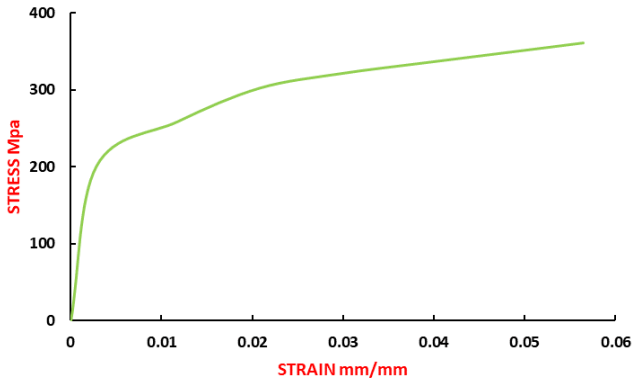


**Fig. 2. Stress versus strain curves used in the FE models.**

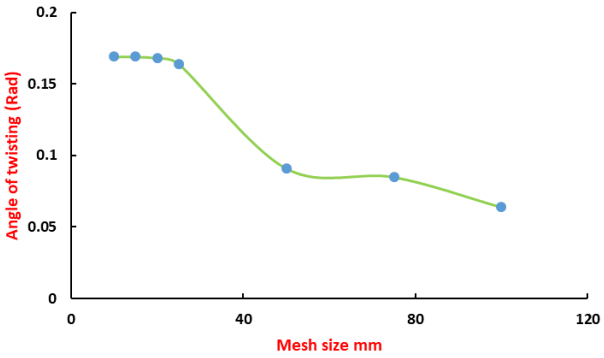


**Fig. 3. Convergent study for mish size.**

### 3.2. Calibration of models

The results of earlier researchers [14] and the author's earlier work in the torque-twisting angle response, ultimate torque, and failure mode were utilized in the process of calibrating the finite-element model. To calibrate the torque-twisting angle response of the square hollow section steel beam model, a tensile strength parameter was considered. This factor had a significant impact on the results and behavior of all models, as the failure load and the yield stress depended greatly on it. The findings of FE are significantly impacted by this parameter and steel module, according to research that was conducted in the past [15]. The findings of the experiments and the finite element analysis agreed after several tests were conducted since the specimens exhibited the same torque-twisting angle response, as shown in Fig. 5.

A failure mechanism that was identical to the one found in the trials was also detected in the matching FE simulation. A lateral buckling failure occurred in the square hollow section steel beam that was tested and simulated. The failure began at the sidewalls of the beam and subsequently spread to all the beam's components. In addition, the ultimate torque of the calibrated specimens was compared to the torque of the test specimens that had been experimentally examined by the researchers who came before. Since the difference between the experimental and FE ultimate torque ranged less than 18%, the FE model was found to be more conservative than the experiment. The torque-twisting angle response and ultimate torque capacity were utilized to validate the calibrated models. It was noted that there was a good concordance in the elastic and plastic phases.

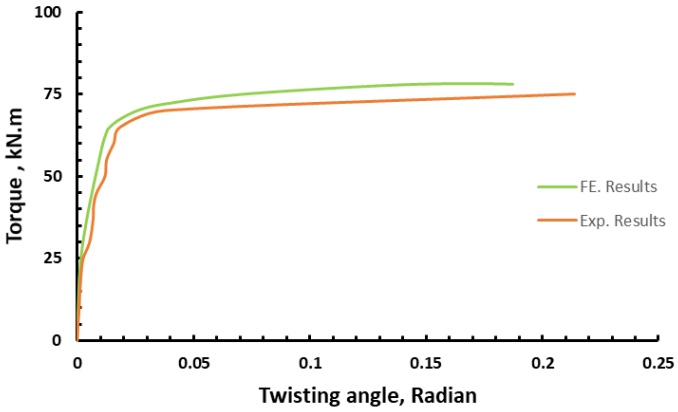


**Fig. 5. Experimental results Vs. finite elements results.**

## 4. Results and Discussions

### 4.1. Load- displacement correlation

Figure 6 displays the torque–twisting angle curve for every square hollow steel section (SHS) beam type. Two steps may be seen in the torque–twisting angle response when examining the model. The applied force and the resultant twisting angle in the first phase are proportionate along a straight line. This was the point at which the torque–twisting angle curve sharply declined. The torque-twisting angle curve changes form as

the torque rises to the maximum failure value, indicating that the SHS beam has entered a plastic phase. Since a little increase in charge results in a significant rise in the twisting angle, altering the slope of the torque–twisting angle curve causes the specimens' plastic zone to quickly expand. The addition of holes often alters the behavior of the SHS beam, causing the elastic stage to drop and the twisting angle to rise, which causes the models to fail ductile. This is due to the increased amount of elongation in the models, especially around the openings.

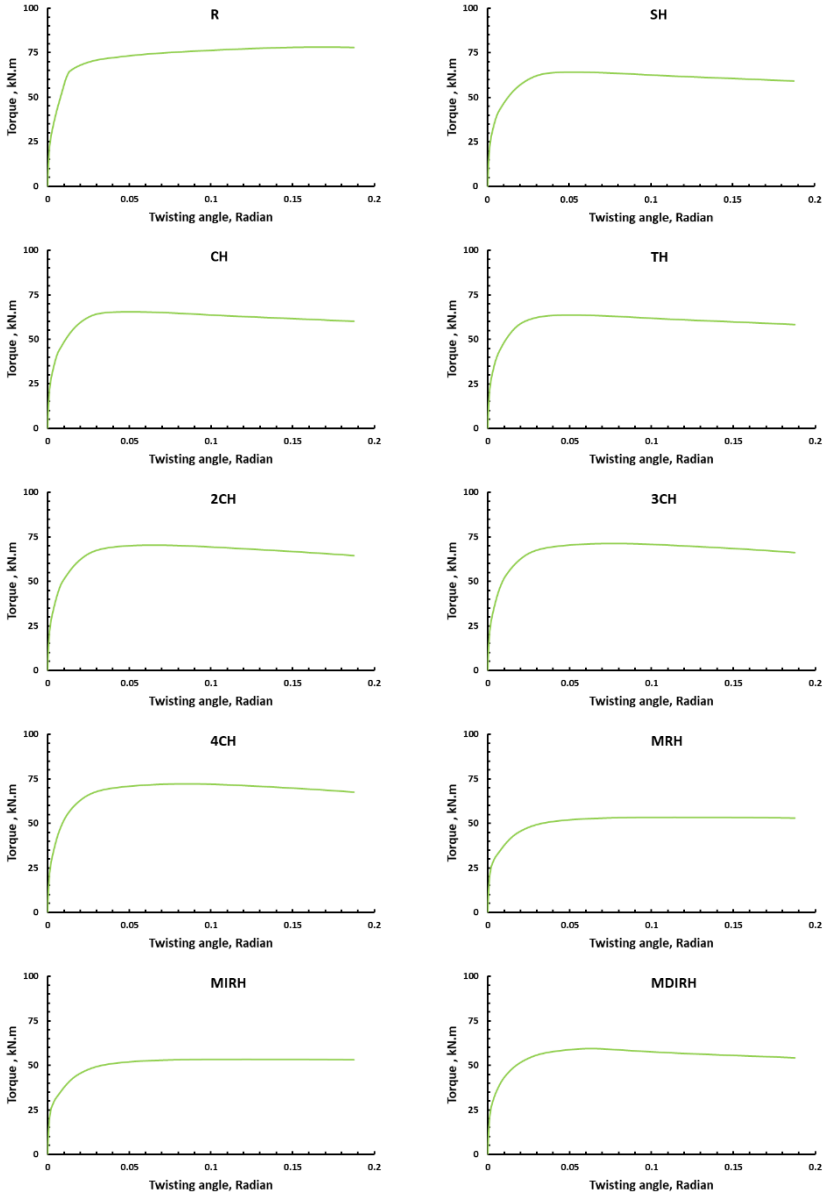


**Fig. 6. Torque-twisting angle curves for models.**

## 4.2. Failure torque and failure twisting angle

To find the maximum torque strength and investigate other parameters affecting the behavior of square steel beams, models with various hole shapes and numbers were simulated. This study was conducted on models with triangular, circular, and rectangular holes. To determine the maximum torque strength, models with two, three, and four circular holes are also included. For every form, the hole area was kept at 40,000 square millimeters. In addition, the model's weight was reduced by adding successive longitudinal, inclined and crossed openings. About 14% of the model's weight was reduced when using vertical and inclined openings, while when using crossed openings, the model's weight was reduced by about 18%.

Table 2 shows the study results. It is clear that the ultimate torque decreased significantly between 16 and 18 % when the hole was added to the model. This lowers because the existence of the hole causes weak spots in the beam. Additionally, the maximum torque strength of the beam remains same when the hole's form is changed from rectangular to triangular, however it is somewhat increased when a circular hole is used.

The rectangular and triangular hole shapes have comparable effects on the ultimate torque strength, as seen by the roughly stale and consistent stress distribution around the hole. When two circles are used to create an equivalent area of a circular form, the ultimate torque of the SHS beam is reduced by 10% compared to the reference beam's strength. Additionally, it is reduced by around 8.7% and 7.6% compared to employing three and four circles, respectively.

When successive vertical and inclined slots were used to reduce the models' weight, the torsional strength was reduced by about 31% compared to the reference model. When the slots intersected, the strength was reduced by about 24%. This indicates that the intersecting slots have better torsional strength, which may be due to the stress dispersion on the section due to the cross-sectional shape.

The failure twisting angle decreases hugely when there are holes in the SHS beam due to a decrease in the failure torque of models. After examining the models with the successive vertical and inclined holes, however, it is found that the specimen's twisting angle has grown significantly. All models have twisting angles that are less than the reference model.

**Table 2. Results of the study.**

| Specimen Designations | Torque (kN.m) | $\frac{TR-T}{TR} \times 100$, % | Twisting angle (Radian) | $\frac{\theta R-\theta}{\theta R} \times 100$, % | Reduction in Weight of Models, % |
|---|---|---|---|---|---|
| R | 78.3 | --- | 0.167 | --- | 0.0 |
| SH | 64.0 | -18.3 | 0.051 | - 69.5 | 2 |
| CH | 65.5 | - 16.3 | 0.051 | - 69.5 | 2 |
| TH | 63.7 | - 18.6 | 0.050 | - 70.0 | 2 |
| 2CH | 70.3 | - 10.2 | 0.064 | - 61.7 | 2 |
| 3CH | 71.5 | - 8.7 | 0.078 | - 53.3 | 2 |
| 4CH | 72.3 | - 7.6 | 0.085 | - 49.1 | 2 |
| MRH | 53.3 | - 31.9 | 0.115 | - 31.1 | 14 |
| MIRH | 53.4 | - 31.8 | 0.126 | - 24.6 | 14 |
| MDIRH | 59.3 | - 24.3 | 0.063 | - 63.3 | 18 |

TR: Torque of reference model, T: Torque of any model.
$\theta R$: Twisting angle of the reference model, $\theta$: Twisting angle of any model.

### 4.3. Models' failure mechanism and failure mode

Figure 7 shows that the presence of perforation significantly affected the stress distribution pattern. Although the unperforated member exhibited a similar stress distribution over all four faces, it was observed that the stress pattern on the perforated face differed from the stress pattern on the other unperforated faces. The tension in the perforated part was concentrated around its perimeter, in contrast to the uniform distribution of tension in the unperforated member. All thin members failed as a local buckling near halfway the length of the unperforated member or at the outer boundary of the perforation in the perforated member. Compared to the unperforated member, a reduced torsional capacity was found for the perforated member. This might mean that the perforated face is not doing a good job resisting torsional force since stress relaxation exists except around the perimeter of the perforation.

In general, failure starts from the middle of the square hollow steel section beam and then extends in the section. The areas surrounding the holes are affected first, reaching the yield stage at failure. As for the multi-holes found in the section to reduce weight, the steel generally did not reach yield when the holes were vertical and inclined but reached it when the holes were in the form of intersections. This is due to the increasing torsional capacity of models.

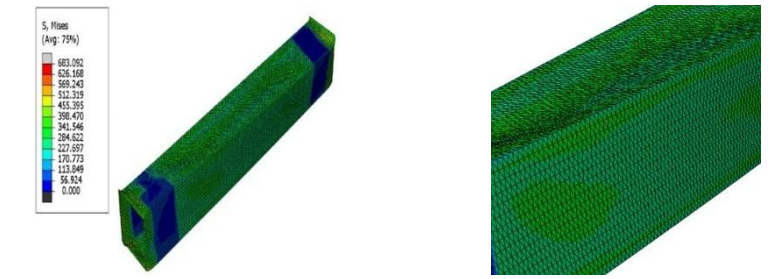


**R**

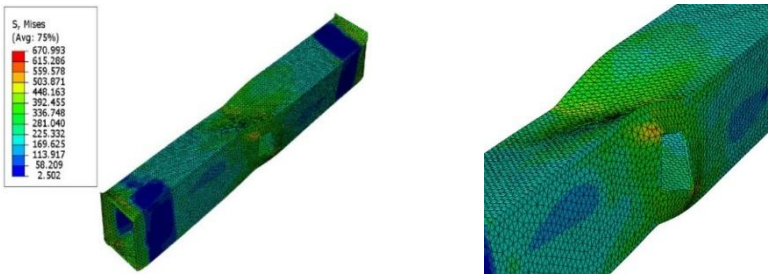


**SH**

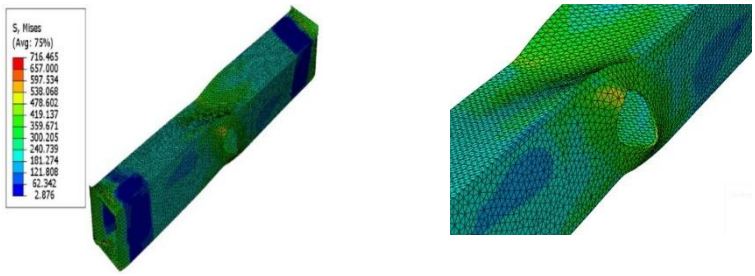


**CH**

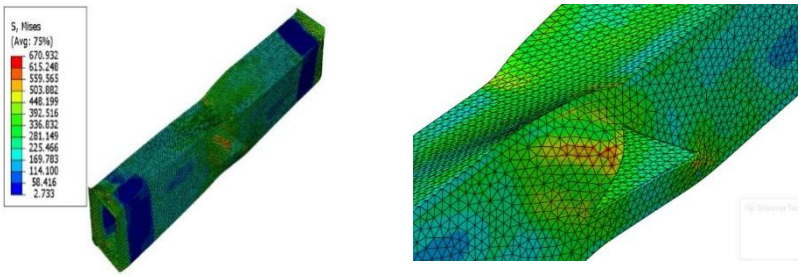


**TH**

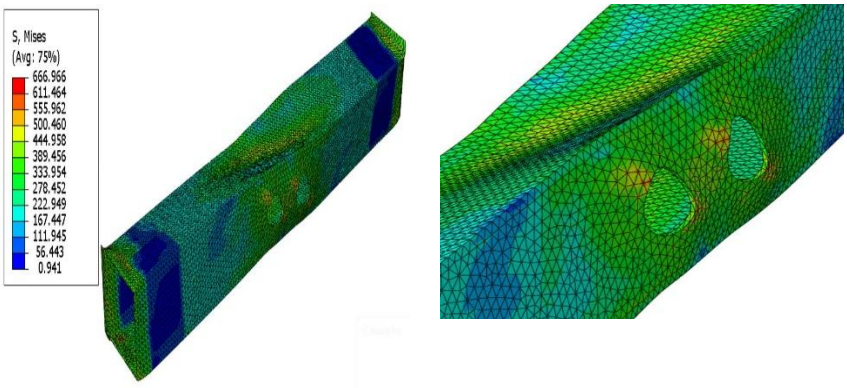


**2CH**

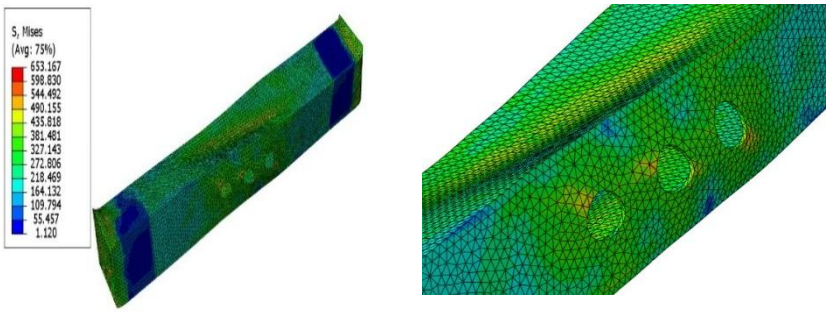


**3CH**

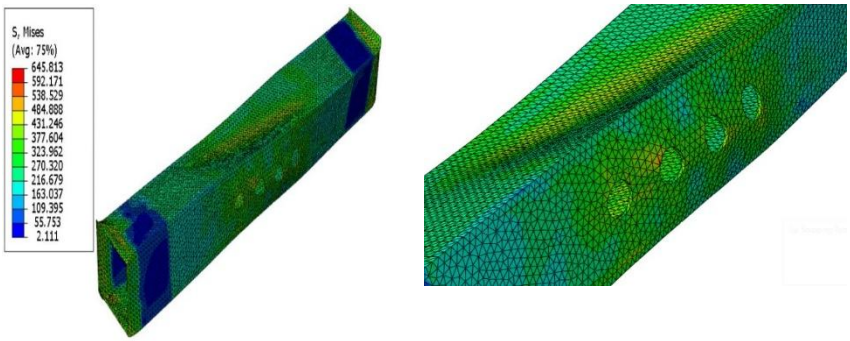


**4CH**

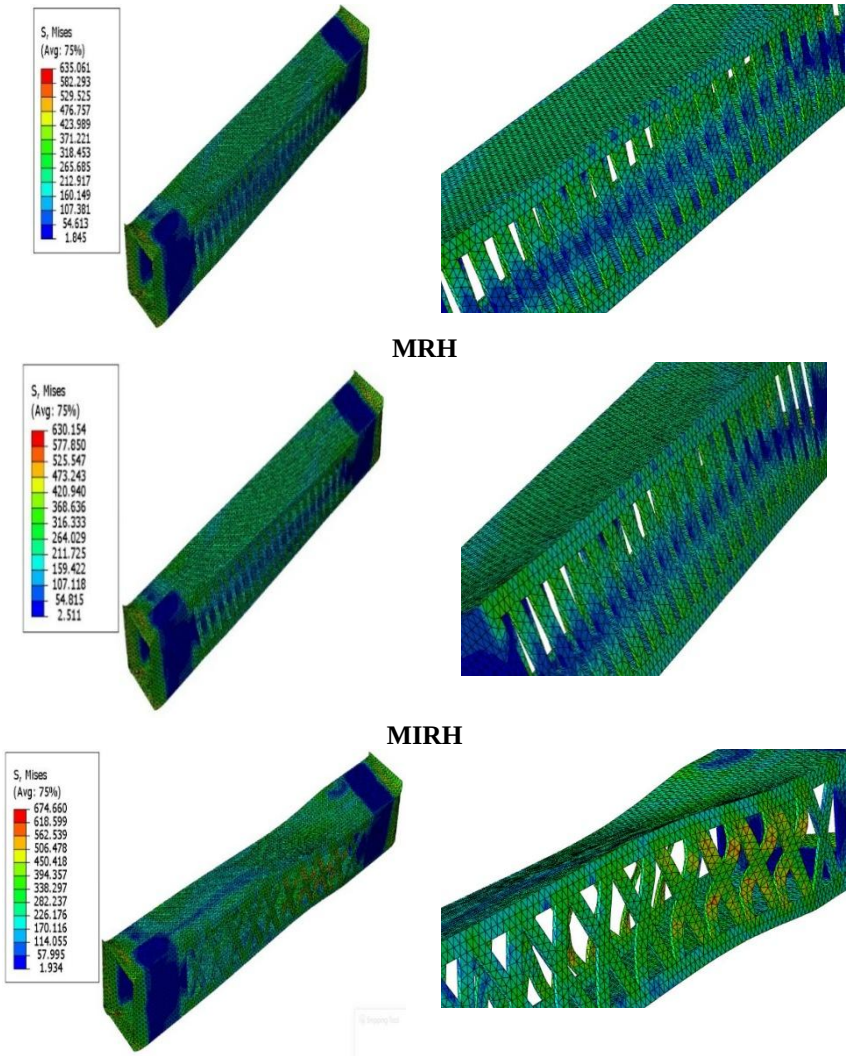


**Fig. 7. Failure mode of FE models.**

## 5. Conclusion

In the context of this investigation, the following conclusions might be taken based on the findings obtained from the finite-element simulation using the ABACUS technique for steel beam models with a square hollow section that was subjected to a two-torsional load:

- Concerning the torque-twisting angle response, failure mode, and ultimate torque capacity, the 3D finite element model utilized in this study can simulate the square hollow section steel beam. Additionally, it agrees with the simulation.
- The numerical analysis was shown to have a high level of validity when compared to the experimental data. The most remarkable difference ratio based

on the ultimate torque was found to be less than 18% for all of the models that were studied using numerical analysis.

- The existence of holes in the square hollow section steel beam significantly impacts the overall ultimate torsional strength of the model and its general behaviour.
- The ultimate torsional strength of the model is 18% lower than the reference model when square and triangle holes are added to it. On the other hand, the ultimate strength experiences a 16% drop when circular holes are added to the model. Based on these findings, it is clear that the circular form is advantageous when it comes to creating apertures.
- When the area of one circular hole is replaced by two, three or four circular holes, the maximum torsional strength is reduced by 10, 8 and 7% of the strength of the reference model, respectively. This shows that distributing the area over more than one circular hole improves the torsional performance of the models.
- The weight of the specimens can be reduced by adding successive openings on both sides, as this reduction helps manufacture steel sections.
- Compared to the reference model, the model's weight was reduced by 14% when successive longitudinal and inclined apertures were introduced. Additionally, the ultimate torsional strength of the model was lowered by 31.9%.
- The weight of the specimen was reduced by 18% by adding crossed openings, and the ultimate torsional strength was reduced by 24% compared to the reference model. This indicates that crossed openings are better at resisting torsional forces than vertical openings.
- The failure mode is usually local buckling failure for all models.

For future studies, the effect of different opening shapes, such as diamond-shaped on the ultimate strength can be studied. Also, more considerable weight reductions and their effect on the results can be studied.

## Acknowledgements

The researchers thank all their colleagues who participated in the scientific research.

## References

1. Rahman, A.A.A.; and Shallal, A.S. (2017). Research article enhancing torsional behaviour of cold formed square hollow steel columns by carbon fibre reinforced polymer. *Research Journal of Applied Sciences, Engineering and Technology*, 14(4), 137-145.
2. Sundarraja, M.C.; Sriram, P.; and Prabhu, G.G. (2014). Strengthening of hollow square sections under compression using FRP composites. *Advances in Materials Science and Engineering*, 2014(1), 396597.
3. Mahendran, M.; and Keerthan, P. (2013). Experimental studies of the shear behavior and strength of LiteSteel beams with stiffened web openings. *Engineering Structures*, 49, 840-854.

4. Devi, S.V.; and Singh, K.D. (2020). Finite element study of the stiffening effects on torsional capacity of perforated stainless steel slender semi-elliptical hollow section members. *Structures*, 26, 66-78.
5. Wanniarachchi, K.S.; Mahendran, M.; and Keerthan, P. (2017). Shear behaviour and design of lipped channel beams with non-circular web openings. *Thin-Walled Structures*, 119, 83-102.
6. Ridley-Ellis, D.J.; Owen, J.S.; and Davies, G. (2003). Torsional behaviour of rectangular hollow sections. *Journal of Constructional Steel Research*, 59(5), 641-663.
7. Pham, C.H. (2017). Shear buckling of plates and thin-walled channel sections with holes. *Journal of Constructional Steel Research*, 128, 800-811.
8. Pellegrino, C.; Maiorana, E.; and Modena, C. (2009). Linear and non-linear behaviour of steel plates with circular and rectangular holes under shear loading. *Thin-Walled Structures*, 47(6-7), 607-616.
9. Pham, S.H.; Pham, C.H.; and Hancock, G.J. (2017). Direct strength method of design for channel sections in shear with square and circular web holes. *Journal of Structural Engineering*, 143(6), 04017017.
10. Devi, S.V.; Singh, T.G.; and Singh, K.D. (2019). Cold-formed steel square hollow members with circular perforations subjected to torsion. *Journal of Constructional Steel Research*, 162, 105730.
11. Abaqus, Abaqus/Standard user's Manual Volumes I-III and ABAQUS CAE Manual. (2009). Providence, USA.
12. Khamees, A.A.; and Shadhan, K.K. (2021). Experimental investigation of dendriform structure under static loading. *Journal of Applied Science and Engineering*, 24(1), 57-64.
13. Khamees, A.A.; Tameemi, W.A.; Al-Rammahi, A.A.; and Sulaiman, E.A. (2024). Enhancing load capacity: a numerical investigation of corrugated steel beams with web holes. *Journal of Engineering Science and Technology*, 19(3), 762-773.
14. Mosheer, K.A.-M.; and Almusawi, J.N. (2023). Experimental study of steel box beams strengthened by steel truss under torsion. *Civil Engineering and Architecture*, 11(5), 2676-2686.
15. Hussein, H.H.; Walsh, K.K.; Sargand, S.M.; Rikabi, F.T.A.; and Steinberg, E.P. (2017). Modelling the shear connection in adjacent box-beam bridges with ultrahigh-performance concrete joints. I: Model calibration and validation. *Journal of Bridge Engineering*, 22(8), 04017043.